Vol 16 No 8, August 2007
1009-1963/2007/16(08)/2180-08

Chinese Physics

© 2007 Chin. Phys. Soc.
and IOP Publishing Ltd

The acoustoelastic effect on Rayleigh waves in elastic–plastic deformed layered rocks*

Liu Jin-Xia(刘金霞)†, Cui Zhi-Wen(崔志文), and Wang Ke-Xie(王克协)

Department of Acoustics and Microwave Physics, School of Physics, Jilin University, JieFang Road 2519, Changchun 130021, *China*

(Received 28 November 2006; revised manuscript received 16 January 2007)

On the basis of the acoustoelastic theory for elastic–plastic materials, the influence of statically deformed states including both the elastic and plastic deformations induced by applied uniaxial stresses on the Rayleigh wave in layered rocks is investigated by using a transfer matrix method. The acoustoelastic effects of elastic–plastic strains in rocks caused by static deformations, are discussed in detail. The Rayleigh-type and Sezawa modes exhibit similar trends in acoustoelastic effect: the acoustoelastic effect increasing rapidly with the frequency-thickness product and the phase velocity change approaching a constant value for thick layer and high frequency limit. Elastic–plastic deformations in the Castlegate layered rock obviously modify the phase velocity of the Rayleigh wave and the cutoff points for the Sezawa modes. The investigation may be useful for seismic exploration, geotechnical engineering and ultrasonic detection.

Keywords: acoustoelastic, Rayleigh wave, elastic–plastic
PACC: 0340K, 4630J, 9165

1. Introduction

The acoustoelastic effect, i.e. the velocity change of the acoustic wave in the presence of stresses, has been investigated for more than 50 years.[1] Residual stresses, externally applied stresses and strains can all lead to a change in propagation velocity of a wave, such as a bulk wave, Rayleigh wave, Love wave and Lamb wave.[2−4] Many scientists[2,4] have investigated the acoustoelastic effects on the Rayleigh waves propagating in the layered Ge/Si systems. Those researches are mainly stimulated by interest in the nondestructive evaluation of third-order elastic constants and/or residual stresses in metal samples. In the research, the residual stresses are mainly induced by the mismatching of material properties between film and substrate. The residual stresses are induced by a variety of sources, and one of the sources is plastic deformation.[5] In seismic reservoir characterization, the effects of stresses and plastically yielded rocks are more recognized. Generally, the elastic wave velocity increases with the increase of compressive stress applied to sedimentary rocks. However, as the applied stress exceeds a yield stress and approaches a value of failure, the material undergoes an elastic–plastic deformation prior to mechanical failure, and the elastic wave velocity starts to decrease.[6] Wave propagation in rocks subjected to elastic–plastic deformations can be described by the equations of motion for small dynamic fields superposed on a static bias.[6,7] The static bias refers to the statically deformed state of the material with large deformations. The bulk wave propagation along a principal stress direction has been described in terms of total static strain and plastic strain.[6] Whereas the layered structures are often detected in seismic exploration, geotechnical engineering and ultrasonic detection,[8−16] for example, the road surface of speedway, groundwork, etc, the layered structures may undergo elastic and plastic deformations induced by applied stresses. Experiments[17−19] have shown that the nonlinear response of sedimentary rocks subjected to applied stresses is more obvious than that of other media. Therefore, it is significant to study the influence of elastic and plastic deformations induced by applied stresses on the Rayleigh wave in layered rocks.

The Rayleigh waves have been widely investigated[13−16] to determine the material parameters in geophysics, geotechnical engineering and ultrasonic detection. Some studies have shown the sen-

*Project supported by the National Natural Science Foundation of China (Grant Nos 10534040 and 40674059) and the Specialized Research Fund for Doctoral Program of Higher Education of China (Grant No 20040183045).
†Corresponding author. E-mail: cuizw@jlu.edu.cn; ljxjlu@sina.com

sitivity of this wave to stress in different materials.[20] How the statically deformed states including the elastic and plastic strains induced by applied stresses influence the velocities of the Rayleigh waves in the layered rocks, we do not know. In this paper, we attempt to investigate the acoustoelastic effect on the Rayleigh wave for the Castlegate layered rock with elastic and plastic deformations induced by uniaxial stresses deposited on the Berea substrate. On the basis of the acoustoelastic theory for elastic–plastic materials,[6,7] we study the influence of the elastic and plastic strains caused by static deformations on the Rayleigh wave propagation in layered rocks by using a transfer matrix method.[2] The material is isotropic in the absence of static deformations in this paper.

This paper is organized as follows. In Section 2, we describe the wave propagation in an elastic–plastic continuum. In Section 3, we describe the Rayleigh wave for the Castlegate layered rock deposited on the Berea substrate. In Section 4, the numerical results are displayed and discussed. The obtained results may arouse the interest of researchers in the above-mentioned fields and also in the experimental wave propagation in elastic–plastic deformed media.

2. Acoustoelastic theory for elastic–plastic materials

Following the acoustoelastic theory for elastic–plastic materials proposed by Johnson[7] and Sinha and Plona[6], a primary variable E^{p}_{AB} is introduced and referred to as the plastic strain, to which the following properties are assigned: 1) it is a symmetric tensor, 2) it has the same invariance properties as the total strain, 3) when the stress is removed from a material point, the plastic strain equals the total strain, and 4) the constitutive relation for the rate of change of plastic strain is independent of time scale. When the applied loading produces a stress that exceed a yield stress, a permanent (or plastic) deformation occurs in the material. The elastic–plastic deformation of the material in the biased state is assumed to take place in an isothermal process. It is also assumed that the plastic deformation does not make any contribution to the Helmholtz free energy. It is further assumed that the small-amplitude wave propagation does not cause any additional plastic deformation beyond the propagation region exists a statically deformed state. Three configurations of the body: reference, intermediate (deformation), and current configuration, play a crucial role in the theory. We choose the intermediate (deformation) configuration to describe the wave propagation in a rock with elastic–plastic deformations. Let the vectors $\boldsymbol{X}$, $\boldsymbol{x}$ and $\boldsymbol{x}^{\mathrm{c}}$ with components X_A, x_i and x^{c}_i represent the reference, intermediate and current states, respectively. A subscript comma denotes partial differentiation with respect to $\boldsymbol{X}$ or $\boldsymbol{x}$, depending on the following subscript, and summation convention holds for the repeated subscripts and also for those capitalized subscripts.

Equations of motion in intermediate coordinates are

$$\partial \left[\left(C_{ijkl} + T_{il}\delta_{kj} \right) u_{k,l} \right] / \partial x_i = \tilde{\rho}\ddot{u}_j, \tag{1}$$

where

$$C_{ijkl} = \left[\tilde{\rho}/\rho_0 \right] F_{iA}F_{jB}F_{kC}F_{lD} \left(c_{ABCD} + c_{ABCDEF}E^{\mathrm{e}}_{EF} \right), \tag{2}$$

$$T_{il} = \left[\tilde{\rho}/\rho_0 \right] F_{iA}F_{lB} \left(c_{ABCD}E^{\mathrm{e}}_{CD} + \frac{1}{2}c_{ABCDEF}E^{\mathrm{e}}_{CD}E^{\mathrm{e}}_{EF} \right), \tag{3}$$

$$\tilde{\rho} \cong \rho_0 \left(1 - E^{\mathrm{t}}_{NN} \right), \tag{4}$$

$$2E^{\mathrm{t}}_{AB} = F_{iA}F_{iB} - \delta_{AB}, \tag{5}$$

$$E^{\mathrm{e}}_{AB} = E^{\mathrm{t}}_{AB} - E^{\mathrm{p}}_{AB}, \tag{6}$$

$$F_{iA} = x_{i,A}, \tag{7}$$

Equation (1) represents the equation of an infinitesimal motion in a deformed elastic–plastic medium. It is interesting that the form of this expression is the same as that for a small dynamic field applied to a statically elastic bias.[5] However, the stiffness tensor $\boldsymbol{C}$ and the Cauchy stress tensor $\boldsymbol{T}$ in the intermediate state are functions of the plastic strain and

work hardening.[7] u_i is the small dynamic displacement, the dot denotes the differentiation with respect to time, F_{iA} denotes the static deformation gradient, c_{ABCD} and c_{ABCDEF} are the second-order and third-order elastic constants[5] respectively. Isotropic material has two independent second-order elastic constants and three independent third-order elastic constants. E^{t}_{AB} is the total static strain. The superscripts e and p denote the elastic and plastic components, and $\tilde{\rho}$ and ρ_0 are the mass density in intermediate and reference states, respectively. Equations (2) and (3) are nonlinear in the elastic and total strains. Similar relation derived from the usual acoustoelastic theory[5,21] has been presented for infinitesimal strains so that the velocities can be linearized. In deriving a theory for a finite elastic–plastic deformation, such a linearization may or may not be appropriate.[7]

3. The Rayleigh wave in a stressed layer on a substrate

The physical model is shown in Fig.1. A stressed layer is deposited on a substrate. Half the space noted with '0' is the Berea substrate, and the part denoted with '2' is vacuum. The layer labelled with '1' is the Castlegate layered rock. The $x_3 = 0$ plane in the Cartesian coordinate system is the interface between the layer and the substrate while the plane $x_3 = -h$ is the free surface of layer. For applied stresses we

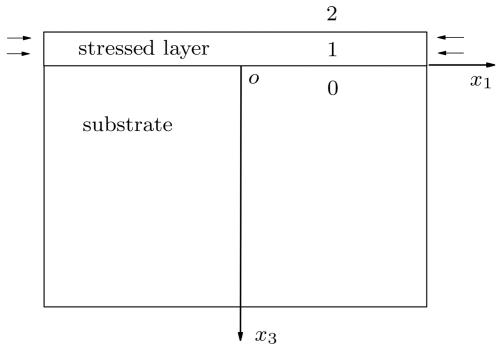


Fig.1. The geometry of the problem considered and corresponding coordinate system.

assume the uniaxial model, with axial strain components being $E^{\mathrm{t}}_{11} = E^{\mathrm{e}}_{11} \neq 0$ and $E^{\mathrm{t}}_{22} = E^{\mathrm{e}}_{22} = E^{\mathrm{t}}_{33} = E^{\mathrm{e}}_{33}$ in the absence of any plastic strains in the material, and $E^{\mathrm{t}}_{11} \neq 0$, $E^{\mathrm{t}}_{22} = E^{\mathrm{t}}_{33}$ and $E^{\mathrm{e}}_{11} = E^{\mathrm{t}}_{11} - E^{\mathrm{p}}_{11}$, in the presence of plastic strains in the material.[6] Assuming the plane-wave propagation to be in the direction perpendicular to x_2, i.e. $\partial u_i/\partial x_2 = 0$, we have homogeneous static strains induced by applied stress within the layer, i.e. $E^{\alpha}_{ij}(x_1, x_2, x_3) = E^{\alpha}_{ij}$, where $\alpha = \mathrm{t}, \mathrm{e}, \mathrm{p}$. Since the reference state is selected to be isotropic in the absence of applied stresses, the transverse displacement u_2 is decoupled from u_1 and u_3. Voigt's notation may be used to indicate the indices of stiffness tensors C_{ijkl}, c_{ABCD} and c_{ABCDEF} ($11\rightarrow 1, 22\rightarrow 2, 33\rightarrow 3, 23\rightarrow 4, 13\rightarrow 5, 12\rightarrow 6$), and the stiffness tensors can be written as C_{pq}, c_{pq} and c_{pqr} ($p, q, r = 1, 2, \ldots, 6$).[6] Then the wave propagation in the system can be described by equation of motion for the prestressed layer

$$
\begin{aligned}
&(C_{11} + T_{11})\frac{\partial^2 u_1}{\partial x_1^2} + C_{13}\frac{\partial^2 u_3}{\partial x_1 \partial x_3} + C_{55}\frac{\partial^2 u_1}{\partial x_3^2} + C_{55}\frac{\partial^2 u_3}{\partial x_3 \partial x_1} = \tilde{\rho}\frac{\partial^2 u_1}{\partial t^2},\\
&C_{13}\frac{\partial^2 u_1}{\partial x_3 \partial x_1} + C_{33}\frac{\partial^2 u_3}{\partial x_3^2} + (C_{55} + T_{11})\frac{\partial^2 u_3}{\partial x_1^2} + C_{55}\frac{\partial^2 u_1}{\partial x_1 \partial x_3} = \tilde{\rho}\frac{\partial^2 u_3}{\partial t^2}.
\end{aligned} \tag{8}
$$

The constitutive equation in the intermediate coordinates can be obtained from Refs.[6,7]

$$\sigma^c_{ij} = T_{ij} + C_{ijkl}e_{kl} + u_{i,k}T_{kj}, \tag{9}$$

where σ^c_{ij} is the first Piola–Kirchhoff stress tensor in an intermediate configuration, $e_{kl} = (u_{k,l} + u_{l,k})/2$ is the elastic strain due to a small-amplitude wave propagation. In this paper the applied stresses are the uniaxial model along the x_1-direction, the Cauchy stress components T_{i3} are set to be zero, and the first Piola–Kirchhoff stress components perpendicular to the interface are

$$\sigma^c_{i3} = C_{i3kl}e_{kl}, \quad i = 1, 3. \tag{10}$$

We now consider the Rayleigh wave moving in the direction of the x_1-axis

$$u_i(x_1, x_3) = B_i \mathrm{e}^{-bkx_3}\mathrm{e}^{\mathrm{i}(kx_1 - \omega t)}. \tag{11}$$

Substituting the expression(11) into to Eq.(8), we obtain

$$\begin{bmatrix} -(C_{11}+T_{11})+\tilde{\rho}c^2+C_{55}b^2 & -\mathrm{i}b(C_{13}+C_{55}) \\ -\mathrm{i}b(C_{13}+C_{55}) & -(C_{55}+T_{11})+\tilde{\rho}c^2+C_{33}b^2 \end{bmatrix} \begin{bmatrix} B_1 \\ B_3 \end{bmatrix} = 0 \tag{12}$$

for the Rayleigh wave, the existence condition of non-trivial solutions for B_1 and B_3 is that the determinant in Eq.(12) vanishes, which yields a four-order algebraic equation in b, with velocity c use as the parameter, i.e. $A_1b^4 + A_2b^2 + A_3 = 0$, where

$$\begin{aligned} A_1 &= C_{55}C_{33}, \\ A_2 &= C_{33}\left(-C_{11}-T_{11}+\tilde{\rho}c^2\right) \\ &\quad +C_{55}\left(-C_{55}-T_{11}+\tilde{\rho}c^2\right)+(C_{13}+C_{55})^2, \\ A_3 &= \left(-C_{11}-T_{11}+\tilde{\rho}c^2\right)\left(-C_{55}-T_{11}+\tilde{\rho}c^2\right). \end{aligned} \tag{13}$$

From the above equation, the four roots b_g (g =1,2,3,4) of b can be obtained. In addition, from Eq.(12), each b_g ($g = 1, 2, 3, 4$) yields the amplitude ratio β_g, i.e.

$$\beta_g = \frac{B_{3g}}{B_{1g}} = \frac{\mathrm{i}(C_{13}+C_{55})b_g}{-C_{55}-T_{11}+\tilde{\rho}c^2+C_{33}b_g^2}. \tag{14}$$

Then the displacements may be expressed as

$$\begin{aligned} u_1 &= \sum_{g=1}^{4} B_{1g}\mathrm{e}^{-kb_gx_3}\mathrm{e}^{\mathrm{i}(kx_1-\omega t)}, \\ u_3 &= \sum_{g=1}^{4} \beta_g B_{1g}\mathrm{e}^{-kb_gx_3}\mathrm{e}^{\mathrm{i}(kx_1-\omega t)}. \end{aligned} \tag{15}$$

From the expression (15) and the constitutive relations (10), one can write the formal solutions for the displacements and stresses in matrix form as follows:

$$\boldsymbol{\nu}_1(x_3) = \boldsymbol{D}_1\boldsymbol{R}_1(x_3)\boldsymbol{B}, \tag{16}$$

where

$$\begin{aligned} \boldsymbol{\nu}_1 &= [u_1 \;\; u_3 \;\; \sigma_{33}^c \;\; \sigma_{13}^c]^{\mathrm{T}}, \\ \boldsymbol{D}_1 &= \begin{bmatrix} 1 & 1 & 1 & 1 \\ \beta_1 & \beta_2 & \beta_3 & \beta_4 \\ \mathrm{i}kC_{13}-kb_1\beta_1C_{33} & \mathrm{i}kC_{13}-kb_2\beta_2C_{33} & \mathrm{i}kC_{13}-kb_3\beta_3C_{33} & \mathrm{i}kC_{13}-kb_4\beta_4C_{33} \\ kC_{55}(-b_1+\mathrm{i}\beta_1) & kC_{55}(-b_2+\mathrm{i}\beta_2) & kC_{55}(-b_3+\mathrm{i}\beta_3) & kC_{55}(-b_4+\mathrm{i}\beta_4) \end{bmatrix}, \\ \boldsymbol{R}_1(x_3) &= \begin{bmatrix} \mathrm{e}^{-kb_1x_3} & 0 & 0 & 0 \\ 0 & \mathrm{e}^{-kb_2x_3} & 0 & 0 \\ 0 & 0 & \mathrm{e}^{-kb_3x_3} & 0 \\ 0 & 0 & 0 & \mathrm{e}^{-kb_4x_3} \end{bmatrix}, \quad \boldsymbol{B} = [B_{11} \;\; B_{12} \;\; B_{13} \;\; B_{14}]^{\mathrm{T}}. \end{aligned} \tag{17}$$

It is well known that the major disturbance of the Rayleigh wave motion is restricted to the region near the surface, which requires that the components of displacement tend to zero when x_3 approaches to infinite. Therefore, only two roots of b' with positive real parts can be selected. The superscript ' ′ ' represents the corresponding quantities associated with the substrate. Thus the displacement and stress vectors of the substrate can be expressed as

$$\boldsymbol{\nu}_0(x_3) = \boldsymbol{D}_0 \begin{bmatrix} 0 \\ B'_{12}\mathrm{e}^{-kb'_2x_3} \\ 0 \\ B'_{14}\mathrm{e}^{-kb'_4x_3} \end{bmatrix}. \tag{18}$$

Here, $\boldsymbol{D}_0$ can be obtained by substituting the elastic constants c'_{13}, c'_{33}, c'_{55} and ρ' of the isotropic substrate into Eq.(17). Expressions (16)–(18) have the same features as those for the transfer-matrix approach with

the static elastic strains induced by residual stresses.[2] Hence the numerical procedure for the solution is similar to that for the stressed[2] or unstressed body. One can establish the transfer matrix $\boldsymbol{P}_1(-h,0)$ to relate the displacements and stresses at the lower surface of the layer '1' to those at the upper surface according to Eq.(16) as follows:

$$\boldsymbol{\nu}_1(-h) = \boldsymbol{P}_1(-h,0)\,\boldsymbol{\nu}_1(0), \tag{19}$$

and

$$\boldsymbol{P}_1(-h,0) = \boldsymbol{D}_1\boldsymbol{R}_1(-h)\,\boldsymbol{D}_1^{-1},$$

where $\boldsymbol{\nu}_1(-h)$and $\boldsymbol{\nu}_1(0)$are respectively the vectors at the upper and lower surfaces of the layer '1'. Equation (18) at $x_3 = 0$ becomes

$$\boldsymbol{\nu}_0(0) = \boldsymbol{D}_0(0)\,(0, B'_{12}, 0, B'_{14})^{\mathrm{T}}. \tag{20}$$

The displacements and stresses must be continuous across the interface between layer '1' and the substrate '0', i.e.

$$\boldsymbol{\nu}_1(0) = \boldsymbol{\nu}_0(0). \tag{21}$$

From Eqs.(18–21), the displacements and stresses vectors at the top of layer '1' can be written as

$$\boldsymbol{\nu}_1(-h) = \boldsymbol{G}\,(0, B'_{12}, 0, B'_{14})^{\mathrm{T}}, \tag{22}$$

where

$$\boldsymbol{G} = \boldsymbol{P}_1(-h,0)\,\boldsymbol{D}_0(0).$$

For the free surface, i.e. the surface of layer '1', we have

$$\sigma^c_{\mathrm{i}3}(x,-h) = 0, \quad i = 1,3. \tag{23}$$

By substituting Eqs.(22) into the boundary conditions (23), we obtain

$$\begin{pmatrix}\sigma_{33}\\ \sigma_{13}\end{pmatrix} = \begin{pmatrix}G_{32} & G_{34}\\ G_{42} & G_{44}\end{pmatrix}\begin{pmatrix}B'_{12}\\ B'_{14}\end{pmatrix} = \begin{pmatrix}0\\ 0\end{pmatrix}, \tag{24}$$

Equation (24) has nontrivial solutions when the determinant is equal to zero. the phase velocity equation is thus obtained as follow:

$$G_{32}G_{44} - G_{34}G_{42} = 0. \tag{25}$$

4. Numerical results

In this section, we apply the transfer matrix method to the calculation of the Rayleigh wave. In particular, we will discuss the influence of the elastic–plastic strains induced by static deformations on the Rayleigh wave within a Castlegate layered sandstone deposited on a Berea sandstone. Linear and nonlinear constants for rocks are listed in Table 1.

Table 1. Linear and nonlinear constants for sandstones.

	$\rho_0/(\mathrm{kg/m^3})$	$V_p/(\mathrm{m/s})$	$V_s/(\mathrm{m/s})$	c_{144}/GPa	c_{456}/GPa	c_{123}/GPa
Castlegate	2000	2000	2000	−162.5	−340.8	−95.9
Berea	2135	3022	3022	—	—	—

The unconfined compressive strength of the Castlegate sandstone is 16 MPa.[6] According to Ref.[6], in Fig.2 we also assume that the growth in the plastic strains for the Castlegate rock is in the form of a quadratic polynomial in the axial strain E^{t}_{11}, in addition, we do not consider any creeps in the material. The assumed growth is somewhat arbitrary and can cause a slightly larger difference between the predicted and measured velocities at intermediate stresses. Whereas the actual form of the polynomial depends on the used rocks and their loading history, and the experimental data on this very weak Castlegate sandstone indicates that the plastic deformation starts rather early in the first load cycle. Since the reference state is selected to be isotropic in the absence of applied stress and the hysteretic behaviour is not considered to be caused by frictional losses during static deformation, the lateral strains $E^{\mathrm{t}}_{22} = E^{\mathrm{t}}_{33} = -\nu E^{\mathrm{t}}_{11}$. The poisson's ratio ν is given by $\left(V_p^2 - 2V_s^2\right)/2\left(V_p^2 - V_s^2\right)$. The previous work[22] on elastic–plastic deformation of weak sandstones under uniaxial loading shows that ν_{plastic} is roughly one-tenth of ν_{elastic}. In this paper, we use the Poisson ratio, $\nu_{\mathrm{plastic}} = 0.1\nu_{\mathrm{elastic}}$, to calculate the transverse plastic strains in terms of axial plastic strain. In order to investigate the influence of elastic and elastic–plastic strains induced by static deformations on the phase velocity and the penetration behaviour, we have a total static strain of the Castlegate sandstone, $E^{\mathrm{t}}_{11} = -0.002$, and plastic strains, $E^{\mathrm{p}}_{11} = -0.000625$ (see Fig.2) in the existence of plastic strain and $E^{\mathrm{t}}_{11} = E^{\mathrm{e}}_{11} = -0.002$ in the absence of

plastic strain induced by applied stresses, besides, we introduce a phase velocity shift of $\Delta V = V^{\text{new}} - V$, where V and V^{new} are the phase velocities for the system without and with applied unaxial stresses respectively.

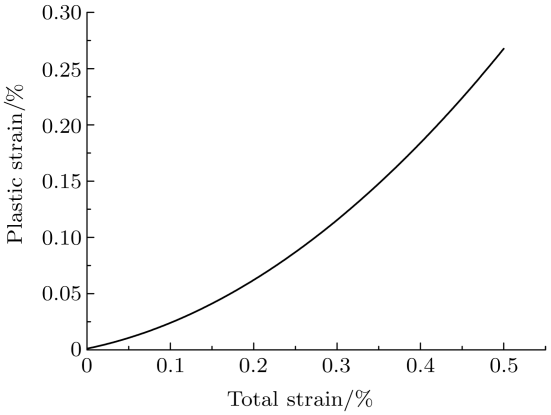


Fig.2. Assumed growth of the plastic strain as a function of total strain in the first load cycle. (from Ref.[6]).

In Fig.3 the phase velocity dispersions of the Rayleigh-type and Sezawa modes with propagation parallel to the -x_1 are shown. Figure 3(a), 3(b) and 3(c) correspond to the unstressed state, statically elastic and elastic–plastic deformations induced by applied stresses in a Castlegate layered rock, respectively. The solid and dashed curves represent linear and nonlinear results in elastic and total strains, respectively. In Fig.3(a) there are six modes for $fh \leq 5000\,\text{m/s}$ in the unstressed layered system. The first mode is the Rayleigh-type mode, and the others are the higher-order Rayleigh modes, i.e. Sezawa modes. For a very thin layer, the Rayleigh wave is mainly determined by the elastic properties of substrate. When the layer thickness h or the operating frequency f increases, the Castlegate layer slows down the velocity until the Rayleigh-type wave is completely localized within the layer finally. Furthermore, each of the high-order Rayleigh modes, i.e. Sezawa modes, has a low-frequency cutoff, at which the phase velocity is equal to the substrate shear velocity, and requires a minimum layer thickness to propagate at a given frequency. In Fig.3(b) one finds only four modes for $fh \leq 5000\,\text{m/s}$ in the Castlegate layered sandstone subjected to statically elastic deformation. The results indicate that the Sezawa modes shift towards high frequencies and the phase velocities are changed compared with those of unstressed state. However, in Fig.3(c) one can find five modes for $fh \leq 5000\,\text{m/s}$ when the Castlegate layer undergoes statically elastic–plastic deformation, which is different from those in both the Figs.3(a) and 3(b), and shows that the Sezawa modes shift towards low frequencies and the phase velocities are obviously changed compared with those of statically elastic deformation. Note that the difference between the 'linear' and 'nonlinear' results is rather small for such strain magnitudes in Figs.3(b), (c). In order to investigate the influences of elastic and elastic–plastic strains induced by applied uniaxial stresses on the Rayleigh wave, the first and second modes are studied in detail.

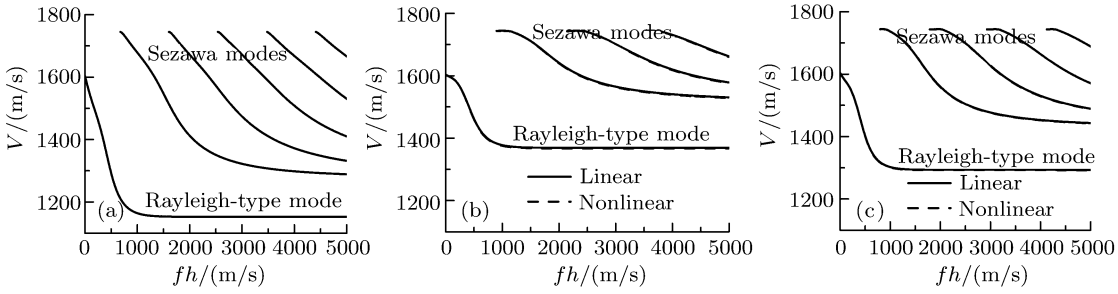


Fig.3. Phase velocity dispersion vs frequency-thickness product fh for the Rayleigh-type and Sezawa modes propagating parallel to the x_1. (a), (b) and (c) correspond to unstressed state, statically elastic and elastic–plastic deformations induced by applied stresses in a Castlegate layered rock, respectively. The solid and dashed curves represent linear and nonlinear results in elastic and total strains, respectively.

Figure 4 shows the influences of elastic and elastic–plastic deformations induced by applied uniaxial stresses on the Rayleigh-type mode. In Figs.4(a) and 4(b) the phase velocity dispersion and change ΔV are displayed, respectively. Curves labelled with 'unstressed', 'elastic' and 'elastic–plastic' represent phase velocities for unstressed state, elastic and elastic–plastic strains induced by static deformations in a

Castlegate layered rock, respectively. The solid and dashed curves refer to linear and nonlinear results in elastic and total strains, respectively. Figure 4(a) displays that the phase velocity obviously increases compared with that of unstressed state when the Castlegate layered rock undergoes statically elastic deformation, and decreases compared with that of statically elastic deformation when the layered rock undergoes elastic–plastic strains induced by static deformation. In Fig.4(b) it is clearly seen that the acoustoelastic effect is dependent on the penetration depth of the wave. For small values of fh, the wavelength is larger than the layer thickness, and the phase shift is small when the layered rock undergoes both the elastic and elastic–plastic strains. With increasing the values of fh, the wavelength becomes considerably smaller than the layer thickness and the wave is completely restricted to the layered rock with both the elastic and elastic–plastic deformations, the acoustoelastic effect is obviously found and increases rapidly. For the thick layer and high frequency limits, the velocity change approximates a constant value, the almost maximal change in phase velocity is 217 m/s as the product of fh is greater than 1415 m/s when the layered rock undergoes the elastic deformation, and maximal change in phase velocity is about 141 m/s as the product of fh is greater than 1305 m/s when the layered rock undergoes the elastic–plastic deformation. The phase velocity change of the wave propagation in a Castlegate layered rock with elastic–plastic deformation is smaller than that with elastic deformation induced by stresses. Note that difference between the 'linear' and 'nonlinear' results is indistinguishable under such strain magnitudes.

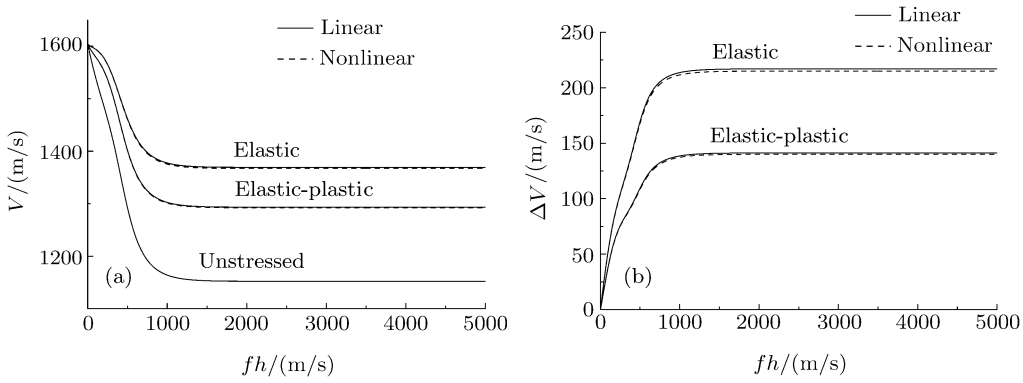


Fig.4. Phase velocity dispersion (a) and change ΔV (b) vs frequency-thickness product fh for the Rayleigh-type wave propagating parallel to the x_1, respectively. Curves labelled with 'unstressed', 'elastic' and 'elastic–plastic' represent phase velocities for unstressed state, statically elastic and elastic–plastic deformations induced by applied stresses in a Castlegate layered rock, respectively. The solid and dashed curves refer to linear and nonlinear results in elastic and total strains, respectively.

Figure 5 shows the influences of elastic and elastic–plastic deformations induced by applied uniaxial stresses on the second mode (Sezawa mode). In Figs.5(a) and 5(b) the phase velocity dispersion V and change ΔV are shown, respectively. The notations are the same as those in Fig.4. Figure 5(a) shows that the cutoff for the second modes takes place at about 675 m/s, 900 m/s and 800 m/s, respectively, when the Castlegate layered rock is in an unstressed state and experiences statically elastic and elastic–plastic strains. Similar to the case of the Rayleigh-type mode, Fig.5(a) displays that the phase velocity obviously increases compared with that of unstressed state when the Castlegate layered rock undergoes statically elastic deformation, and decreases compared with that of statically elastic deformation when the layered rock undergoes statically elastic–plastic deformation. One can find from Fig.5(b) that acoustoelastic effect increases rapidly with the increase of product fh for the layered rock subjected to both the elastic and elastic–plastic deformations. The almost maximal change in phase velocity is 240 m/s as the product of fh is greater than 4200 m/s when the layered rock undergoes the elastic deformation, and is about 152 m/s as the product of fh is greater than 3940 m/s when the layered rock undergoes the elastic–plastic deformation. The phase velocity change of the second mode exceeds that of the Rayleigh-type wave including the elastic and elastic–plastic strains induced by static deformations. Although the change of the other

high-order modes are not shown in this paper, one can find that the acoustoelastic effect of high-order modes (Sezawa modes) exceeds that of the Rayleigh-type wave significantly. Also note that the difference between the 'linear' and 'nonlinear' results is rather small for such strain magnitudes as shown in Fig.5.

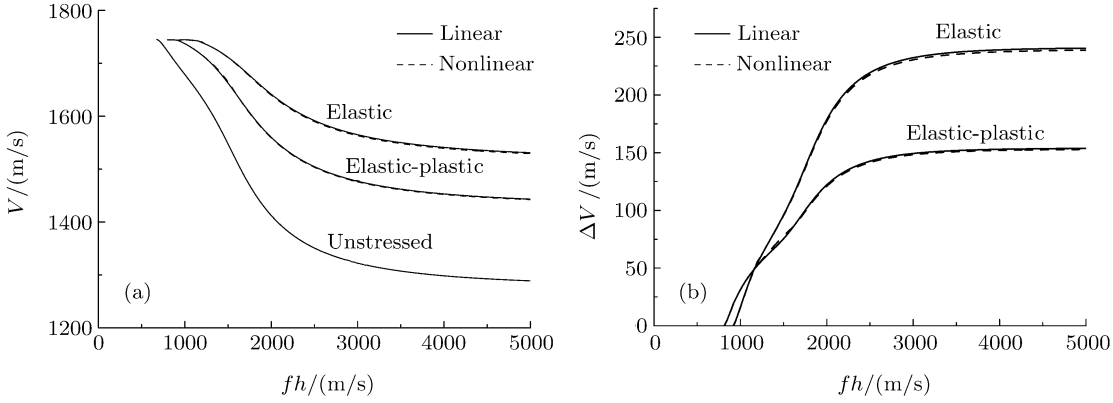


Fig.5. Phase velocity dispersion (a) and chanc ΔV (b) vs frequency-thickness product fh for the second mode (Sezawa) propagating parallel to the x_1. Curves labelled with 'unstressed', 'elastic' and 'elastic–plastic' represent phase velocities for unstressed state, statically elastic and elastic–plastic deformations induced by applied stresses in a Castlegate layered rock, respectively. The solid and dashed curves are for linear and nonlinear results in elastic and total strains, respectively.

5. Conclusions

We have investigated the acoustoelastic effect for the Castlegate layered rock subjected to elastic and elastic–plastic deformations induced by uniaxial stresses. The phase velocity changes of the Rayleigh-type and Sezawa modes due to statically elastic and elastic–plastic deformations reveal a similar trend, and each approximate a constant value, in the thick layer and high frequency limit. However, it is found that the Sezawa modes shift towards high frequencies compared with those of unstressed state, and shift towards low frequencies compared with those of statically elastic deformation. The results show that elastic–plastic deformations in the Castlegate layered rock obviously modify the phase velocity of the Rayleigh wave and the cutoff points for the Sezawa modes, and the phase velocity change in the elastic–plastic deformed layered rocks is smaller than that in the layered rocks only subjected to elastic deformation.

References

[1] Hughes D S and Kelly J L 1953 *Phys. Rev.* **92** 1145
[2] Liu H, Lee J J and Cai Z M 2004 *Mechanics Research Communications* **31** 667
[3] Osetrov A V, Frohlich H J, Koch R and Chilla E 2000 *Phys. Rev.* B **62** 13963
[4] Chilla E, Osetrov A V and Frohlich H J 2001 *Phys. Rev.* B **63** 1133083
[5] Pao Y H, Sachse W and Fukuoka H 1984 *Physical Acoustics*, ed. Mason W Pand Thurston R N (New York: Academic) pp61–143
[6] Sinha B K and Plona T J 2001 *Geophysics* **66** 772
[7] Johnson G C 1981 *J. Acoust. Soc. Am.* **70** 591
[8] Wang Y J, Ning W and Ou X H 1994 *Chin. Phys.* **3** 561
[9] Fokin A V 1997 *Chin. Phys.* **6** 574
[10] Zhang H Y, Liu Z Q and Ma X S 2003 *Acta Phys. Sin.* **52** 2492 (in Chinese)
[11] Xue H H, Liu X Z, Gong X F and Zhang D 2005 *Acta Phys. Sin.***54** 5233 (in Chinese)
[12] Qin B, Chen J J and Cheng J C 2005 *Chin. Phys.* **14** 2522
[13] Zhang B X, Xiong W, Yu M, Lan C Q and Li L 1996 *J. Acoust. Soc. Am.***100** 3527
[14] Zhang B X, Lu L Y and Wang C H 2004 *Chin. Phys. Lett.* **21** 682
[15] Lu L Y, Wang C H and Zhang B X 2006 *Appl. Phys. Lett.* **88** 014101
[16] Lu L Y, Zhang B X and Wang C H 2006 *Chin. J. Geophys.* **49** 1082 (in Chinese)
[17] Johnson P A, Meegan G D, McCall K, Bonner B P and Shankland T J 1992 *J. Acoust. Soc. Am.* **91** 2350
[18] Meegan G. D, Johnson P A, Guyer R A and McCall K R 1993 *J. Acoust. Soc. Am.* **94** 3387
[19] Winkler K W and Liu X Z 1996 *J. Acoust. Soc. Am.* **100** 1392
[20] Marc D, Mohammadi Q, Mohamed Q and Frederic J 2002 *Ultrasonics* **39** 575
[21] Toupin R A and Bernstein B 1961 *J. Acoust. Soc. Am.* **33** 216
[22] Papamichos E and van den Hoek P J 1995 Daemen J J K and Schultz R A Eds *Rock Mechanics*, Proc. 35th U.S. Symp. pp301–306